

Dynamic Transition in Vortex Flow in Strongly Disordered Josephson Junction Arrays and Superconducting Thin Films

Daniel Domínguez

Centro Atómico Bariloche, 8400 S. C. de Bariloche, Rio Negro, Argentina

(Received 16 June 1998)

We study the dynamics of vortices in strongly disordered $d = 2$ Josephson junction arrays and superconducting films driven by a current. We find a dynamic phase transition in vortex flow at a current $I_p > I_c$. Below I_p there is plastic flow characterized by an average-velocity correlation length scale ξ_v in the direction of motion, which diverges when approaching I_p . Above I_p we find a moving vortex phase with homogeneous flow and short range smectic order. A finite-size analysis shows that this phase becomes asymptotically a liquid for large length scales. [S0031-9007(98)08089-2]

PACS numbers: 74.60.Ge, 74.50.+r, 74.60.Ec

The study of nonequilibrium steady states of driven many-degrees-of-freedom systems with quenched disorder are of importance in many condensed matter systems [1–21]. Examples of this problem are the dynamics of vortices in type-II superconductors [1,2] and charge density waves [3]. For low driving forces the dynamics is dominated by disorder leading to a plastic flow regime [1,2,4–6]. On the other hand, for very large driving forces the randomness should be less important and all the internal degrees of freedom will move more or less coherently as a whole [1,2]. Recently, Koshelev and Vinokur [2] have proposed that there is an ordered moving vortex phase. However, Giarmarchi and Le Doussal [7] have shown that some modes of static disorder are still present in the moving system, leading to a moving Bragg glass (MBG) phase [7]. In turn, Balents, Marchetti, and Radzihovsky [8] have argued that the driven state is a moving smectic (MS), consisting of liquid channels with transverse periodic order. Experimentally, studies of current-voltage characteristics [10,11] and neutron-scattering experiments [12] have found a reordering of the vortex structure when increasing the current bias. Recently, Pardo *et al.* [13] have found in decoration experiments that for low magnetic fields there is a MS vortex structure while for high fields there is a MBG. Numerical simulation studies have also found an ordering of the vortex system for high currents [1,2,14–17]. Moon *et al.* [14] have found a MS phase in $d = 2$ molecular dynamics simulations with a short-range interaction potential, while in [17] a MBG phase was found in a driven XY model simulation for $d = 3$ and large magnetic fields. Therefore, questions such as those considering the existence and nature of a moving phase and which effects of the disorder remain once the vortices are in motion are currently under discussion.

Most of the experimental systems mentioned above have the difficulty that there is no control of the nature and amount of disorder. Therefore the study of disordered Josephson junction arrays (JJA) becomes particularly promising here, since they can be specifically fabricated with controlled randomness [18]. For example, questions

such as the dynamics of JJA with percolation disorder [18,19] and the plastic flow of vortices have been studied recently [20]. Also, there is an intrinsic interest in the nonlinear dynamics of JJA and their nonequilibrium properties; see, for example, [21]. In this paper we will show that there is a dynamic transition in driven JJA with strong positional disorder.

The current flowing in the junction between two superconducting islands in a JJA is modeled as the sum of the Josephson supercurrent and the normal current [19–21],

$$I_\mu(\mathbf{n}) = I_\mu^0(\mathbf{n}) \sin \theta_\mu(\mathbf{n}) + \frac{\Phi_0}{2\pi c R_N} \frac{\partial \theta_\mu(\mathbf{n})}{\partial t}, \quad (1)$$

where $I_\mu^0(\mathbf{n})$ is the critical current of the junction between the sites \mathbf{n} and $\mathbf{n} + \boldsymbol{\mu}$ in a square lattice [$\mathbf{n} = (n_x, n_y)$, $\boldsymbol{\mu} = \hat{x}, \hat{y}$], R_N is the normal state resistance, and $\theta_\mu(\mathbf{n}) = \theta(\mathbf{n} + \boldsymbol{\mu}) - \theta(\mathbf{n}) - A_\mu(\mathbf{n}) = \Delta_\mu \theta(\mathbf{n}) - A_\mu(\mathbf{n})$ is the gauge invariant phase difference with $A_\mu(\mathbf{n}) = \frac{2\pi}{\Phi_0} \times \int_{\mathbf{n}\mathbf{a}}^{(\mathbf{n}+\boldsymbol{\mu})\mathbf{a}} \mathbf{A} \cdot d\mathbf{l}$. In the presence of an external magnetic field H we have $\Delta_\mu \times A_\mu(\mathbf{n}) = A_x(\mathbf{n}) - A_x(\mathbf{n} + \mathbf{y}) + A_y(\mathbf{n} + \mathbf{x}) - A_y(\mathbf{n}) = 2\pi f$, $f = Ha^2/\Phi_0$, and a is the array lattice spacing. Here we consider a distribution of critical currents $I_\mu^0(\mathbf{n}) = I_0 \delta_\mu(\mathbf{n}) = I_0 [1 + \delta(\text{RAN} - 1/2)]$ with RAN a random uniform number in $[0, 1]$. We take periodic boundary conditions (p.b.c.) in both directions in the presence of an external current I_{ext} in the y direction in arrays with $L \times L$ junctions. The vector potential is taken as $A_\mu(\mathbf{n}, t) = A_\mu^0(\mathbf{n}) - \alpha_\mu(t)$ where in the Landau gauge $A_x^0(\mathbf{n}) = -2\pi f n_y$, $A_y^0(\mathbf{n}) = 0$, and $\alpha_\mu(t)$ will allow for total voltage fluctuations. With this gauge the p.b.c. for the phases are $\theta(n_x + L, n_y) = \theta(n_x, n_y)$ and $\theta(n_x, n_y + L) = \theta(n_x, n_y) - 2\pi f L n_x$. The condition of a current flowing in the y direction, $\sum_{\mathbf{n}} I_\mu(\mathbf{n}) = I_{\text{ext}} L^2 \delta_{\mu,y}$, determines the dynamics of $\alpha_\mu(t)$ [22]. After considering the conservation of current, $\Delta_\mu \cdot I_\mu(\mathbf{n}) = \sum_{\boldsymbol{\mu}} I_\mu(\mathbf{n}) - I_\mu(\mathbf{n} - \boldsymbol{\mu}) = 0$, we obtain the equations

$$\Delta_\mu^2 \frac{\partial \theta(\mathbf{n})}{\partial t} = -\Delta_\mu \cdot S_\mu(\mathbf{n}), \quad (2)$$

$$\frac{\partial \alpha_\mu}{\partial t} = I_{\text{ext}} \delta_{\mu,y} - \frac{1}{L^2} \sum_{\mathbf{n}} S_\mu(\mathbf{n}), \quad (3)$$

where $S_\mu(\mathbf{n}) = \delta_\mu(\mathbf{n}) \sin[\Delta_\mu \theta(\mathbf{n}) - A_\mu^0(\mathbf{n}) - \alpha_\mu]$, we have normalized currents by I_0 and time by $\tau_J = 2\pi c R_N I_0 / \Phi_0$, and we have defined the discrete Laplacian $\Delta_\mu^2 \theta(\mathbf{n}) = \theta(\mathbf{n} + \hat{\mathbf{x}}) + \theta(\mathbf{n} - \hat{\mathbf{x}}) + \theta(\mathbf{n} + \hat{\mathbf{y}}) + \theta(\mathbf{n} - \hat{\mathbf{y}}) - 4\theta(\mathbf{n})$. These same equations represent the dynamics of a superconducting thin film (STF) after discretization of a time-dependent London model. One starts with the current density as the sum of supercurrent and normal current:

$$\begin{aligned} \mathbf{J} &= \mathbf{J}_S + \mathbf{J}_N, \\ \mathbf{J} &= \frac{ie\hbar}{m^*} [\Psi^* \mathbf{D} \Psi - (\mathbf{D} \Psi)^* \Psi] \\ &+ \frac{\sigma \Phi_0}{2\pi c} \frac{\partial}{\partial t} (\nabla \theta - \frac{2\pi}{\Phi_0} \mathbf{A}), \end{aligned} \quad (4)$$

with $\mathbf{D} = \nabla + i\frac{2\pi}{\Phi_0} \mathbf{A}$ and $\Psi(\mathbf{r}) = |\Psi(\mathbf{r})| \exp[i\theta(\mathbf{r})]$. One takes the discretization $\mathbf{r} = (n_x \xi, n_y \xi) = \xi \mathbf{n}$ with the rule $D_\mu \Psi(\mathbf{r}) \rightarrow \frac{1}{\xi} \{\Psi(\mathbf{n} + \boldsymbol{\mu}) - \exp[-i\frac{2\pi}{\Phi_0} \times \mathbf{A}_\mu(\mathbf{n})] \Psi(\mathbf{n})\}$. After considering conservation of current, and assuming $|\Psi(\mathbf{n})|$ is quenched and depends only on disorder, one obtains the same equations as in (2) and (3). Now $I_\mu(\mathbf{n})$ has to be interpreted as current density normalized by $J_0 = 2e\hbar |\Psi_0|^2 / m\xi = \Phi_0 / (8\pi^2 \lambda^2 \xi)$, time normalized by $\tau = c / (4\pi \sigma \lambda^2)$, $\delta_\mu(\mathbf{n}) = |\Psi(\mathbf{n} + \boldsymbol{\mu})| |\Psi(\mathbf{n})| / |\Psi_0|^2$, and the field density is $f = H \xi^2 / \Phi_0 = H / 2\pi H_{c2}$. The $T = 0$ dynamical equations (2) and (3) are solved with a second order Runge-Kutta algorithm with time step $\Delta t = 0.05\tau_J$ and integration time $1000\tau_J$ after a transient of $500\tau_J$. The discrete Laplacian is inverted with a fast Fourier plus tridiagonalization algorithm as in [20].

We consider here very strong disorder with $\delta = 0.5$. For STF, this corresponds to an extremely dense distribution of pinning sites with a pinning potential with a 50% fluctuation in amplitude in the length scale of ξ , while for JJA it corresponds to a 50% fluctuation in the critical currents. The ground state $I_{\text{ext}} = 0$ vortex configuration is a vortex glass with no structure in the structure factor (no Bragg peaks). We study a magnetic field of $f = 1/25$ and system sizes of $L = 50, 100, 150, 200$. We calculate the time average of the total voltage $V = \langle v(t) \rangle = \langle d\alpha_y(t)/dt \rangle$ (normalized by $R_N I_0$) as a function of I as shown in Fig. 1(a) for one sample of size $L = 200$. The error bars of V [obtained from the statistics of the time averaging of $v(t)$] are smaller than the symbol size in Fig. 1(a) (error in $V \sim 10^{-5} - 10^{-4}$). This suggests that the sample size is large enough to be self-averaging. The initial condition is a thermally quenched vortex configuration at $I = 0$. From this state the current I is slowly increased in steps of $\Delta I = 0.01$ taking as an initial condition the last phase configuration of the

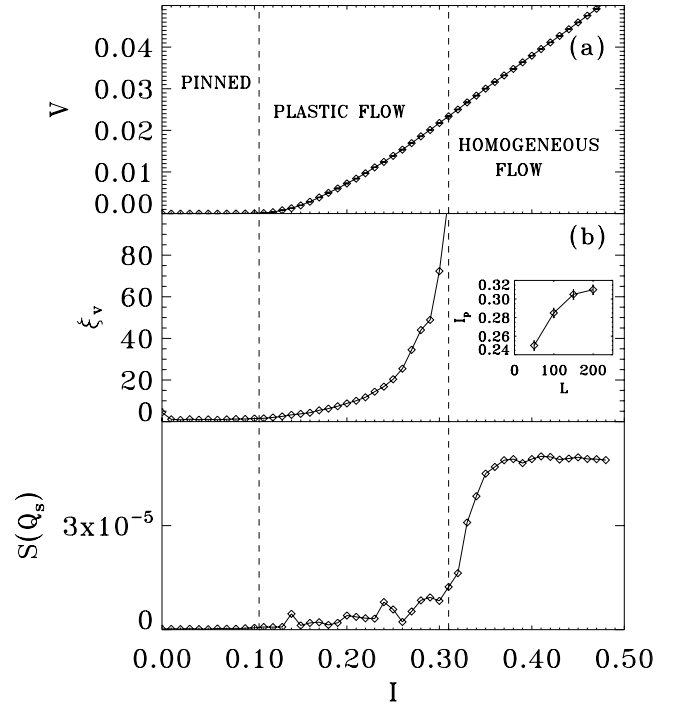


FIG. 1. (a) Voltage vs current for a 200×200 Josephson junction array (or a $200\xi \times 200\xi$ superconducting thin film, STF) with field $f = 1/25$ ($B/H_{c2} = 2\pi/25$ for a STF) and disorder $\delta = 0.5$. (b) ξ_v : Average voltage correlation length along the direction of the Lorentz force; inset: finite-size dependence of I_p . (c) $S(Q_s)$: Intensity of the Bragg peak for smectic order.

previous current. We obtain similar results by slowly decreasing the current from a random vortex configuration at $I = 0.8$. Above a critical current of $I_c = 0.105$ (in units of I_0) there is a nonlinear onset of voltage with a plastic flow of vortices. We study the time-averaged voltage in the bonds parallel to the direction of the current drive: $v_y(\mathbf{n}) = \langle d\theta_y(\mathbf{n}, t)/dt \rangle$, which is proportional to the average vortex speed in the direction of the Lorentz force. We see in Fig. 2(a) that near I_c vortex flow is very inhomogeneous, as typical for the plastic flow regime, showing channels of flow for low currents. For increasing drives the flow becomes more homogeneous as shown in Fig. 2(b). We characterize the inhomogeneity of the flow with the correlation function for voltages along the direction of motion: $C_v(x) = \frac{1}{L^2} \sum_{\mathbf{n}} v_y(\mathbf{n}) v_y(\mathbf{n} + x\hat{\mathbf{x}}) - \langle v_y \rangle^2$. We see in Fig. 2(c) that the voltage correlation increases for increasing values of I . There is a characteristic correlation length ξ_v defined by $C_v(x) \approx C_v(0) \exp(-x/\xi_v)$. This voltage correlation length was proposed by Bhattacharya and Higgins [10] as a characteristic length scale for the dynamics of plastic flow. We see in Fig. 1(b) that ξ_v increases with current I and it diverges ($\xi_v \gg L$) at a current $I_p(L)$. We have also analyzed the voltage correlation function along y , $C_v(y)$. In this case, there is always a fast decay of $C_v(y)$ for any bias current; therefore above I_p the voltage distribution $V_y(\mathbf{n})$ becomes homogeneous

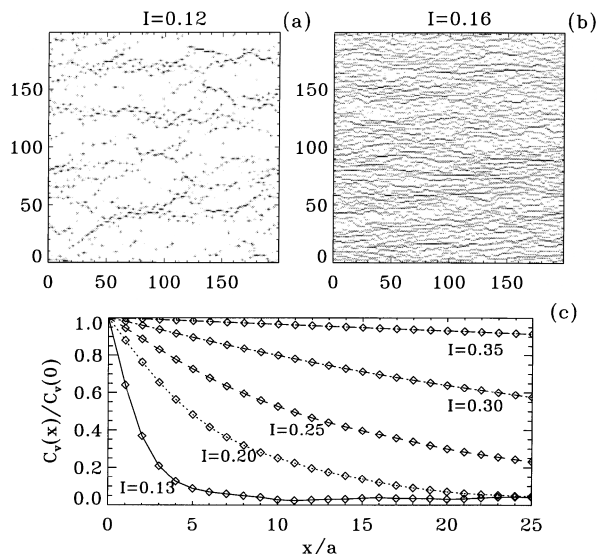


FIG. 2. Time-averaged voltage distribution $v_y(\mathbf{n})$ for low currents in the plastic flow regime. The gray scale is proportional to the voltage intensity. (a) $I = 0.12I_0 \approx 1.2I_c$; (b) $I = 0.16I_0 \approx 1.6I_c$; (c) $C_v(x)$: correlation function of the average voltage along the direction of vortex motion.

along the x direction, but it always has fluctuations along the y direction. This reflects the fact that for large drives the effect of the disorder potential becomes negligible only along the direction of the Lorentz force, but along the transverse direction it is still important [7,8]. The size dependence of $I_p(L)$ is shown in the inset of Fig. 1(b). We see that in the limit of large L , I_p tends to a finite value of $I_p \approx 0.31$ in this case. This shows that in the thermodynamic limit there is a *dynamic phase transition*.

Above I_p , we study the ordering of the moving vortex structure. In order to follow the vortex positions directly, we obtain the vorticity at the plaquette $\tilde{\mathbf{n}}$ (associated with the site \mathbf{n}) as $b(\tilde{\mathbf{n}}) = -\Delta_\mu \times \text{nint}[\theta_\mu(\mathbf{n})/2\pi]$ with $\text{nint}[x]$ the nearest integer of x . We calculate the time-averaged vortex structure factor as $S(\mathbf{k}) = |\langle \frac{1}{L^2} \sum_{\tilde{\mathbf{n}}} \times b(\tilde{\mathbf{n}}) \exp(i\mathbf{k} \cdot \tilde{\mathbf{n}}) \rangle|^2$. For currents $I < I_p$, $S(\mathbf{k})$ has only the density peak $S(\mathbf{k} = 0) = f^2$ and an isotropic ring-like structure as expected for plastic flow [14–16]. On the other hand, for $I > I_p$ there are well-defined peaks in $S(\mathbf{k})$ as shown in the surface plot of Fig. 3(a) for $L = 150$. We see that there are two strong peaks in the k_y direction, at vectors $\mathbf{K} = \pm Q_s \hat{y}$, consistent with smectic ordering in the direction transverse to motion [8]. [$Q_s = 2\pi/a_s$ with $a_s \approx 4.5 \approx (\sqrt{3}/2f)^{1/2}$ the row spacing in a triangular lattice.] There are also small satellite peaks in the other \mathbf{K} directions. The position of the peaks is better seen in the two dimensional gray scale plot of Fig. 3(b). We see that the strongest spots besides $\mathbf{K} = \pm Q_s \hat{y}$ are at the reciprocal space \mathbf{K} vectors corresponding to a triangular lattice, suggesting the presence of some orientational order [23]. In Fig. 3(c) we show a finite-size analysis of $S(Q_s) \sim L^{-\nu_s}$. For a moving smectic with quasi-long-range order one ex-

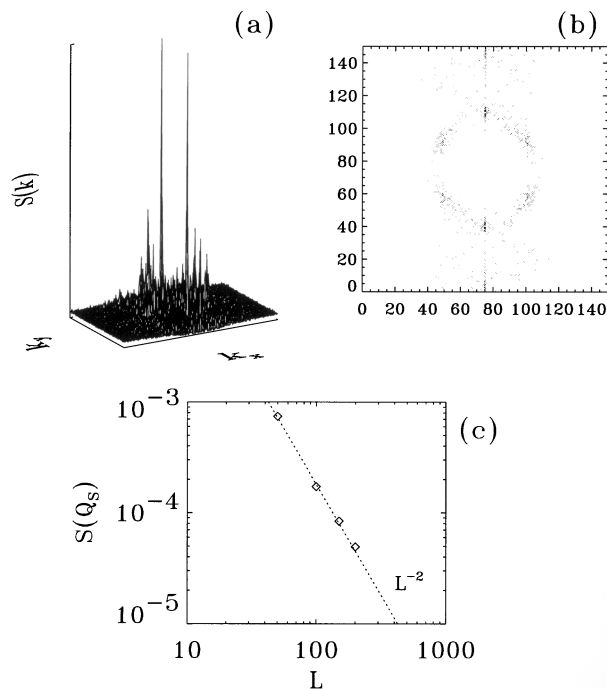


FIG. 3. (a) Surface intensity plot of the structure factor $S(\mathbf{k})$ of the moving vortex system for a current $I = 0.40I_0 \approx 4I_c$ and $L = 150$. We set the central peak $S(0) = 0$ for clarity. (b) Gray-scale intensity of $S(\mathbf{k})$. (c) Finite-size analysis of the smectic order $S(Q_s)$.

pects $\nu_s < 2$, while $\nu_s = 2$ is the value for a liquid. We obtain $\eta_s = 1.96 \pm 0.06 \approx 2$. Therefore in the thermodynamic limit vortex flow is always liquidlike in nature for sufficiently large length scales, and smectic ordering is only a short-range phenomenon in $d = 2$, at least for strong disorder. This is consistent with renormalization group calculations which find that a moving smectic phase might be unstable in $d = 2$ [8]. In Fig. 1(c) we show the parameter of short-range smectic order $S(Q_s)$ as a function of I for a lattice size $L = 200$. We find that for large drives $S(Q_s)$ is nearly current independent, it decreases when decreasing I , and it vanishes when approaching I_p from above. This confirms the result that there is a dynamic transition at I_p where there is an onset of anisotropic short-range order.

The “flux flow noise” has been studied in many current-voltage measurements [24,25]. Here we analyze the voltage noise response with the power spectrum $P(\nu) = |\frac{1}{T} \int_0^T dt v(t) \exp(i2\pi\nu t)|^2$. We find that in the plastic flow regime, very near to I_c , the power spectrum shows $1/\nu$ noise; see Fig. 4(a). On the other hand, for large drives $I > I_p$, the power spectrum tends to a frequency independent value for $\nu \rightarrow 0$ as shown in Fig. 4(b). These two types of power spectra for $I < I_p$ and $I > I_p$ have also been found in the experiments [24,25].

In conclusion, we find a dynamic phase transition at a current I_p above the critical current I_c . This transition is between two different types of liquids which differ in

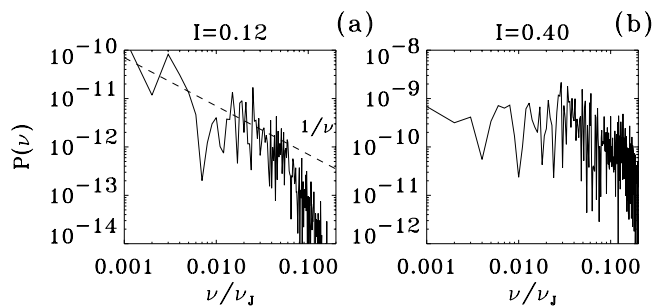


FIG. 4. Voltage power spectrum $P(\nu)$, with frequencies normalized by $\nu_J = \frac{\Phi_0}{2\pi c R_N I_0}$ (for a STF, $\nu_J = 4\pi\sigma\lambda^2/c$). (a) $I = 0.12I_0 \approx 1.2I_c$. (b) $I = 0.40I_0 \approx 4.0I_c$.

their *dynamics* and the spatiotemporal nature of the flow. Below I_p there is a plastic flow regime (“turbulent”) with an isotropic liquid structure. The inhomogeneity of the flow is characterized by a finite average-voltage correlation length [10]. Above I_p there is a regime with homogeneous flow in the direction of motion (“laminar”) and with a structure with anisotropic short-range order. Finite-size analysis shows that moving smectic order is only a short-range phenomenon in $d = 2$ [8]. These moving vortex phases could be observable experimentally in Josephson junction arrays using vortex-imaging techniques.

D.D. acknowledges Fundación Antorchas and Conicet (Argentina) for financial support.

Note added in proof.—In a recent preprint, I. S. Aranson, S. Scheidl, and V. M. Vinokur, cond-mat/9805400, have shown that in $d = 2$ the topological order of driven vortex lattices is always destroyed on large length scales.

- [1] A.-C. Shi and A. J. Berlinsky, Phys. Rev. Lett. **67**, 1926 (1991).
- [2] A. E. Koshelev and V. M. Vinokur, Phys. Rev. Lett. **73**, 3580 (1994).
- [3] L. Balents and M. P. A. Fisher, Phys. Rev. Lett. **75**, 4270 (1995).
- [4] H. J. Jensen *et al.*, Phys. Rev. Lett. **60**, 1676 (1988); A. E. Koshelev, Physica (Amsterdam) **198C**, 371 (1992); F. Nori, Science **271**, 1373 (1996); C. Reichhardt *et al.*, Phys. Rev. Lett. **78**, 2648 (1997).
- [5] N. Grønbech-Jensen, A. R. Bishop, and D. Domínguez, Phys. Rev. Lett. **76**, 2985 (1996).

- [6] C. J. Olson, C. Reichhardt, and F. Nori, Phys. Rev. Lett. **80**, 2197 (1998).
- [7] T. Giamarchi and P. Le Doussal, Phys. Rev. Lett. **76**, 3408 (1996); P. Le Doussal and T. Giamarchi, Phys. Rev. B **57**, 11 356 (1998).
- [8] L. Balents, M. C. Marchetti, and L. Radzihovsky, Phys. Rev. B **57**, 7705 (1998).
- [9] S. Scheidl and V. M. Vinokur, Phys. Rev. B **57**, 13 800 (1998).
- [10] S. Bhattacharya and M. J. Higgins, Phys. Rev. Lett. **70**, 2617 (1993); Phys. Rev. B **52**, 64 (1995).
- [11] M. C. Hellerqvist *et al.*, Phys. Rev. Lett. **76**, 4022 (1996).
- [12] U. Yaron *et al.*, Nature (London) **376**, 743 (1995).
- [13] F. Pardo *et al.*, Phys. Rev. Lett. **78**, 4633 (1997); Nature (London) (to be published).
- [14] K. Moon, R. T. Scalettar, and G. Zimányi, Phys. Rev. Lett. **77**, 2778 (1996).
- [15] S. Ryu *et al.*, Phys. Rev. Lett. **77**, 5114 (1996).
- [16] S. Spencer and H. J. Jensen, Phys. Rev. B **55**, 8473 (1997).
- [17] D. Domínguez, N. Grønbech-Jensen, and A. R. Bishop, Phys. Rev. Lett. **78**, 2644 (1997).
- [18] M. G. Forrester *et al.*, Phys. Rev. Lett. **37**, 5966 (1988); A.-L. Eichenberger *et al.*, Phys. Rev. Lett. **77**, 3905 (1996).
- [19] W. Xia and P. L. Leath, Phys. Rev. Lett. **63**, 1428 (1989); E. Granato and D. Domínguez, Phys. Rev. B **56**, 14 671 (1997).
- [20] D. Domínguez, Phys. Rev. Lett. **72**, 3096 (1994); Physica (Amsterdam) **222B**, 293 (1996); D. Domínguez, N. Grønbech-Jensen, and A. R. Bishop, in *Macroscopic Quantum Phenomena and Coherence in Superconducting Networks*, edited by C. Giovanella and M. Tinkham (World Scientific, Singapore, 1995), p. 278.
- [21] J. S. Chung, K. H. Lee, and D. Stroud, Phys. Rev. B **40**, 6570 (1989); F. Falo *et al.*, Phys. Rev. B **41**, 10983 (1990); N. Grønbech-Jensen *et al.*, Phys. Rev. B **46**, 11149 (1992); P. H. E. Tiesinga *et al.*, Phys. Rev. Lett. **78**, 519 (1997).
- [22] These current-driven p.b.c. were introduced in J. J. Vicente Alvarez, D. Domínguez, and C. A. Balseiro, Phys. Rev. Lett. **79**, 1373 (1997).
- [23] Therefore, the intrinsic pinning by the junctions is irrelevant in this strong disorder and large current case, since the $\delta = 0$, $I_{\text{ext}} = 0$ ground state is a *square* lattice [Y. H. Li and S. Teitel, Phys. Rev. B **47**, 359 (1993)].
- [24] W. J. Yeh and Y. H. Kao, Phys. Rev. B **44**, 360 (1991).
- [25] A. C. Marley *et al.*, Phys. Rev. Lett. **74**, 3029 (1995); R. D. Merithew *et al.*, Phys. Rev. Lett. **77**, 3197 (1996); M. W. Rabin *et al.*, Phys. Rev. B **57**, R720 (1998).